Journal of Sound and Vibration (1998) **217**(2), 335–350
Article No. sv981799

THE USE OF MODAL TAILORING TO MINIMIZE THE RADIATED SOUND POWER OF VIBRATING SHELLS: THEORY AND EXPERIMENT

E. W. Constans, G. H. Koopmann and A. D. Belegundu
Center for Acoustics and Vibrations, The Pennsylvania State University, University Park, PA 16802, *U.S.A.*

(*Received* 30 *June* 1997, *and in final form* 9 *June* 1998)

A numerical design tool is presented for minimizing radiated sound power from a vibrating shell structure using a material tailoring approach. A finite element method using shell elements is used to predict the vibration response of the shell. The sound power generated by the shell under a harmonic force input is computed with a lumped parameter/wave superposition method. A simulated annealing algorithm is used to find optimal point mass distributions for minimum sound power. It is shown that optimal designs are achieved through converting certain mode shapes of the shell into "weak radiators", i.e., modes with low net volume velocities. Close agreement is found between predicted noise levels and experimental measurements, thus providing initial validation of the method as an effective means of finding optimal structural designs for minimum sound power.

1. INTRODUCTION

In contemporary mechanical design, it is becoming more common for the potential noisiness of a machine or structure to be treated as a design consideration. In the design of transportation systems, for example, many of the structures involve thin plates or shells (usually in the form of enclosures) which can be optimized for minimum sound transmission. The design of automobile engines includes sheet-metal valve covers, which protect the rocker-arm/valve assemblies from dirt and seal in lubricating oil. It has long been recognized that the area around the valves is one of the noisiest areas in an engine, due to both combustion noise as well as the impact noise created by the valves in operation. Since valve covers are usually made of relatively thin sheet metal (due to weight and cost considerations) they tend to radiate the engine noise outward from the engine rather than containing it. If a design method were found to convert the valve covers into "weak radiators", that is, structures which vibrate in such a way as to minimize their acoustic power, then automobile engines could be made quieter.

The first part of this paper summarizes some of the current literature in the field of noise reduction and optimization, and demonstrates the need for a fully integrated, structural–acoustic optimization tool. A design methodology is then presented which fills this need, and experimental results are given which show the potential of this new design tool.

0022–460X/98/420335 + 16 $30.00/0

1.1. NOISE-CONTROL-BY-DESIGN

Noise-control-by-design is a design procedure wherein the potential noisiness of a machine is treated as a design consideration. Traditionally, noise control is achieved by integrating large mass, stiffness or damping elements within the structure to minimize vibration and noise. However, in designing modern transportation vehicles, e.g., airplanes or automobiles, weight is at a premium, and consequently more elegant solutions are required. This ultimately leads to the application of optimization strategies.

One of the earliest mentions of the use of optimization to achieve a quiet structure was by Lang and Dym [1], who developed an analytical technique for predicting noise propagation through sandwich panels. The thicknesses and layer densities were used as design variables to achieve optimal transmission losses through the panels. Lamancusa [2] presented a method for optimizing the pipe lengths of an intake manifold system to control low frequency inlet noise on a 4-cylinder automobile engine. In a later work, Milsted *et al*. [3] optimized an engine block for a minimum volume velocity condition by varying panel thicknesses and stiffnesses at connections between engine block subcomponents. In the area of rail transportation, Vincent *et al*. [4] determined optimal values for rail–tie stiffness and rail damping for minimum rolling noise in freight trains through the use of computer simulation.

Noise-control-by-design can be applied to both interior and exterior noise problems. In an enclosure one usually attempts to minimize sound pressure levels globally by maximizing the transmission loss of the enclosing surfaces. In an early paper on the determination of noise levels in interior spaces, Bernhard [5] gave a procedure for calculating the acoustical effects of geometry changes in enclosed cavities. Pal and Hagiwara [6] presented a method of optimization for a coupled structural–acoustic interior noise problem. Specifically, they were interested in solving the ''inverse problem'', that is, finding the minimum change in design variables (e.g., panel thicknesses) which achieve a certain performance criterion. More recently, Engelstad *et al*. [7] reported the use of combined commercial software packages for interior noise minimization. MSC/NASTRAN was used to solve the vibration problem of an acoustically excited aircraft fuselage, and, using the structural vibration as a boundary condition, COMET/Acoustics was used to solve the acoustic problem in the interior. The combination of the two software packages, coupled with an optimizer, is able to find fuselage thicknesses for minimum noise transmission from the engines.

1.2. THE WEAK RADIATOR CONCEPT

One of the most effective means of minimizing the sound power output from a structure is to change a mode shape (or mode shapes) of the structure into a ''weak radiator'' using material tailoring. A weak radiator is a mode which radiates sound very inefficiently due to a correspondingly low net volume velocity. Several recent noise-control-by-design papers have applied this concept, including Belegundu *et al*. [8], St. Pierre and Koopmann [9] and Naghshineh *et al*. [10] All of the preceding researchers used various types of material tailoring to achieve a

weak radiator mode in flat plates or beams. In an interesting twist on the weak radiator concept, Naghshineh and Koopman [11] used active vibration control to *force* a beam to vibrate as a weak radiator. From the successes of the above-cited authors, one may conclude that the weak radiator concept is an effective means of achieving significant noise reductions in vibrating structures. It will be the approach used in this research.

1.3. OPTIMIZATION ALGORITHMS

In most optimization problems, the cost function is either linearly or quadratically dependent upon the design variables; thus, a gradient-based optimization algorithm is the most efficient means to find optimal solutions. However, as noted in a series of papers by Hambric [12–14], gradient-based methods have difficulty optimizing acoustic/structural problems due to their non-linearity, as well as the presence of local minima in the design space. Hambric concluded that non-gradient methods such as the genetic algorithm or the simulated annealing technique should be used in acoustic–structural problems. In an overview of the available structural optimization routines, Keane [15] also found that non-gradient based techniques may have significant advantages over older, gradient-based methods. Further, Szykman and Cagan [16, 17] demonstrated the use of the simulated annealing (SA) algorithm in highly non-linear problems such as three-dimensional routing and component packing. They found that SA was especially effective in problems where the objective function space is discontinuous and/or possesses local minima, a feature which makes the simulated annealing algorithm a logical choice for use in structural/acoustic optimization problems.

A review of the available literature shows that a need exists for a general structural/acoustic optimizer capable of minimizing radiated sound power from three-dimensional structures. Some success has been reported in using a finite element structural response code in conjunction with a boundary element noise prediction code, but it appears as though an integrated, structural sound power minimizer does not yet exist.

The approach taken in this research is to combine a finite element method vibration prediction code with a lumped parameter/wave superposition method for predicting sound power. Upon combining the codes into a single unified package, a simulated annealing algorithm is used to find optimal structural designs from an acoustic power perspective. To the authors' knowledge, this is the first generalized, three-dimensional sound power optimizer for designing thin shell structures. The following sections describe the finite element and lumped parameter/wave superposition codes, followed by a description of the optimization technique. Finally, an example problem is discussed, and comparisons with experimental results are presented.

2. SHELL OPTIMIZATION FOR ACOUSTIC RADIATION

The final result of this research is a computer code called SOAR, which stands for **S**hell **O**ptimization for **A**coustic **R**adiation. SOAR is comprised of two major components: a sound power prediction code and a simulated annealing optimizer

which, in combination, are used to predict, and subsequently minimize noise generated by a vibrating thin shell structure. The shell may be driven at any number of locations and can have fixed, simple-supported or free boundary conditions. If desired, point masses and springs may be attached to nodal locations on the shell. Finally, if the shell covers a sealed mass of air, the stiffness provided by the air can be accounted for in the program.

The sound power prediction program is composed of a vibration prediction section and a noise prediction section. The vibration prediction section uses a finite element method code to predict nodal velocities from a shell driven by a harmonic force. These nodal velocities are then input into the noise prediction section, which uses a boundary element/wave superposition method to predict sound power from the vibrating shell.

2.1. FINITE ELEMENT SECTION

To predict sound power levels from a vibrating shell, it is first necessary to know the velocity at each nodal point on the shell. The finite element code used here employs three-noded, discrete Kirchhoff triangular shell elements. Each node has six degrees of freedom: three translations and three rotations. The stiffness matrix for each element in local co-ordinates is

$$\mathbf{k}' = \begin{bmatrix} \mathbf{k}'_{in\text{-}plane} & & \\ & \mathbf{k}'_{bending} & \\ & & \mathbf{k}'_{\theta z} \end{bmatrix}, \tag{1}$$

where $\mathbf{k}'_{in\text{-}plane}$ represents the plane stress stiffness due to membrane action, $\mathbf{k}'_{bending}$ represents bending stiffness and $\mathbf{k}'_{\theta z}$ is a fictitious stiffness needed when all elements connected to a node are flat. The element mass matrices are given by

$$\mathbf{m}' = \begin{bmatrix} \mathbf{m}'_{in\text{-}plane} & \\ & \mathbf{m}'_{bending} \end{bmatrix}, \tag{2}$$

where

$$\mathbf{m}'_{bending} = \rho t \mathbf{m}'_1 + (\rho t^3/12)\mathbf{m}'_2, \tag{3}$$

ρ being the density of the shell material, t the thickness of the shell, $\mathbf{m}'_1$ is a matrix corresponding to the translational inertia terms and $\mathbf{m}'_2$ is a matrix corresponding to the rotational inertia terms. If one wishes to add point masses to the global stiffness matrix, one may use the equation

$$M_{nn} = M_{nn} + m_n, \tag{4}$$

where m_n is the mass of the point mass. (Refer to Cook [18] and Zienkiewicz [19] for additional details.) To determine the vibration behavior of the shell, one must solve the differential equation

$$\mathbf{M}\ddot{\mathbf{x}} + (\mathbf{K} + \mathrm{i}\mathbf{H})\mathbf{X} = \mathbf{F}, \tag{5}$$

where $\mathbf{X}$ is the nodal displacement vector, $\mathbf{F}$ is the force vector, and

$$\mathbf{H} = \alpha_d \mathbf{K} + \beta_d \mathbf{M} \tag{6}$$

is the damping matrix, and α_d, β_d are damping coefficients. Assuming a hormonic solution, and using modal superposition, the nodal velocities are found to be

$$\dot{\mathbf{X}} = \mathrm{i}\bar{\omega} \sum_{j=1}^{m} y_j \mathbf{Q}^j, \tag{7}$$

where y_j is the modal participation factor, $\bar{\omega}$ is the excitation frequency and $\mathbf{Q}^j$ is the jth eigenvector. The resonance frequencies and mode shapes are determined by solving the eigenvalue problem

$$\mathbf{K}\mathbf{Q}^j = \omega_j^2 \mathbf{M}\mathbf{Q}^j, \tag{8}$$

which is accomplished using the inverse iteration method [20]. The normal (w') components of the nodal velocities are passed on to the sound power prediction portion of the program, which uses them to calculate volume velocities and finally sound power.

2.2. LUMPED PARAMETER/WAVE SUPERPOSITION METHOD

Koopmann *et al*. [21] describe a method of simulating the acoustic radiation of a structure by placing small acoustic point sources in the interior of the structure and matching the volume velocity boundary condition at the surface. Once the strengths of the small sources are known, the total sound power can be found by wave superposition. This enables a continuous structure to be simplified into a lumped parameter model [22] which can be analyzed using numerical methods.

To approximate the acoustic pressure field generated by this collection of simple and dipole sources, the acoustic fields from all of the sources are added together in the following manner:

$$\hat{p}(\mathbf{x}) \approx \sum_{m}^{N} \hat{s}_m P_m(\mathbf{x}). \tag{9}$$

The caret notation indicates the complex amplitude of a function, $\hat{p}(\mathbf{x})$ is the acoustic pressure at the point $\mathbf{x}$, $P_m(\mathbf{x})$ is a basis function describing the pressure field of a single unit acoustic source, and $\hat{s}_m$ is the set of undetermined coefficients which are the strengths for each of the sources.

Since this is a boundary element method, the basis functions must satisfy the governing differential equation (the Helmholtz equation) exactly in the domain, and must satisfy the boundary conditions approximately. The method used here for approximately satisfying the boundary conditions is called volume-velocity matching, and consists of finding the source strengths, $\hat{s}_m$, which cause the volume

velocities over each element to be equal to those given by the finite element code. The volume velocity over an element is defined as

$$\hat{u} = \iint_S \hat{\mathbf{v}} \cdot \mathbf{n} \, \mathrm{d}S, \tag{10}$$

where S is the surface area of an element, $\hat{\mathbf{v}}$ is the velocity over the element, and $\mathbf{n}$ is the unit normal vector to the element. The volume velocity of an element may be thought of as the average normal velocity of the element multiplied by the surface area of the element. For this approximation to the boundary condition to be accurate, the normal velocity over the surface of the element must not vary a great deal, so that it can be approximated as a piston vibrating with a velocity $\hat{\mathbf{v}}_{average}$. Thus, for this method to be accurate, the condition $ka < 1$ should be met, where k is the acoustic wavenumber (ω/c) and a is the largest characteristic dimension of the element.

Euler's equation is now used to rearrange equation (9) into the following form:

$$\hat{\mathbf{v}} \cdot \mathbf{n} \approx \frac{1}{\mathrm{i}k\rho_a c} \sum_m^N \hat{s}_m \nabla P_m(\mathbf{x}) \cdot \mathbf{n}, \tag{11}$$

where ρ_a is the average density of air and c is the speed of sound in air. Integrating over the surface of an element, one writes the elemental volume velocity in terms of the source strengths and basis functions:

$$\hat{u}_n = \iint_{S_n} \hat{\mathbf{v}} \cdot \mathbf{n} \, \mathrm{d}S \approx \frac{1}{\mathrm{i}k\rho_a c} \sum_m^N \hat{s}_m \iint_{S_n} \nabla P_m(\mathbf{x}) \cdot \mathbf{n} \, \mathrm{d}S. \tag{12}$$

To avoid non-uniqueness problems (discussed in much greater detail in the paper by Fahnline and Koopmann [22]) the present basis functions are choosen as the following:

$$P_m(\mathbf{x}) = \alpha((1/R)\, \mathrm{e}^{\mathrm{i}kR}) + \beta\nabla((1/R)\, \mathrm{e}^{\mathrm{i}kR})\mathbf{n}_{q_m}, \tag{13}$$

where R is the distance between a field point $\mathbf{x}$ and the source location $\mathbf{q}_m$, and $\mathbf{n}$ is a vector normal to the acoustic source (that is, normal to the element). The first term in equation (13) represents the acoustic pressure field of a unit simple source, while the second term represents the acoustic field of a dipole source. The coupling constants, α, β determine the relative strengths of the simple and dipole sources. Substituting the basis functions into the volume velocity equation, one writes equation (12) in matrix form,

$$\mathbf{u} = \mathbf{U}\mathbf{s}, \tag{14}$$

where $\mathbf{s}$ is the vector of source strengths. All of the terms in the expression for the $\mathbf{U}$ matrix are known and may be calculated using numerical integration techniques. The volume velocity vector is calculated from the nodal velocities given by the finite element solution. The source strengths of the acoustic sources are

calculated by inverting equation (14). Without going into the details, the power output of a collection of a simple and dipole sources is given by

$$\Pi_{av} = \tfrac{1}{2}\,\mathbf{s}^{H}\mathbf{S}\mathbf{s}, \tag{15}$$

where the superscript H denotes the Hermitian transpose, and the matrix $\mathbf{S}$ is a Hermitian matrix which relates the acoustic power to the source strengths. The elements of the $\mathbf{S}$ matrix are presented in detail in the paper by Fahnline and Koopmann and follow from a derivation by Levine [23, 24].

To summarize, the lumped parameter/wave superposition section of the code first calculates the volume velocities of each element using the nodal velocities provided by the finite element section. The volume velocities provide the needed boundary condition for ultimately predicting sound power with the boundary element method.

2.3. OPTIMIZATION ROUTINE

When choosing an optimization algorithm, one needs to decide whether a gradient or non-gradient routine should be used. Gradient methods have the advantage of (typically) converging on an optimal solution rapidly, especially if the objective function is well-behaved. However, in dynamic problems such as the ones considered in this paper, mode switching can occur, causing the objective function to have "peaks and valleys". Further, in such problems, use of divided differences leads to inaccurate gradient information. Hence, the authors have elected to use a non-gradient algorithm: the simulated annealing technique.

Simulated annealing is a stochastic optimization method. It begins its search at a user-specified design point and then moves in a random direction, searching for a minimum. If the move was in the downhill direction (i.e., if the sound power at the new design is lower than in the original design) the new design is accepted and the algorithm moves again in another random direction. If the move was uphill, however, the new design point has a certain probability of being accepted anyway, depending upon the size of the uphill move and a parameter called the "temperature". In this fashion, the algorithm may escape local minima to converge onto a global minimum.

To understand why the algorithm is called "simulated annealing", consider the annealing process. When a metal is at a high temperature, the atoms within the metal are relatively free to move about in random directions. As the temperature decreases, the atoms become more and more constrained to move within a smaller region, until freezing occurs. Thus, metals find the "optimal" atomic packing by first moving in random directions at high temperatures, with the range of movement decreasing as the temperature decreases. The simulated annealing algorithm works in much the same way, with very large, random steps taken in the beginning, and smaller steps (with less likelihood of uphill steps being accepted) taken as the algorithm proceeds. The simulated annealing algorithm used here is based upon the paper by Corana *et al*. [25].

As design variables in the computer program, one may choose discrete point masses, shell thicknesses, composite properties, to name a few. In this work, point

masses have been chosen as these are simple to build and test in a laboratory to validate the computer simulations.

3. EXAMPLE PROBLEM: OPTIMIZATION OF A HALF-CYLINDRICAL SHELL

To determine the validity of the sound power predictions of SOAR, numerical and physical experiments were undertaken. The optimization problem is an aluminum half-cylinder, mounted on a rigid plate. Figure 1 shows the finite element model of the 2 mm thick half-cylinder, which is 304·8 mm long, with a 158·75 mm inside diameter. The bottom of the half-cylinder is bonded into small grooves in the rigid plate using epoxy, creating a clamped boundary condition. The shell is driven at its top center point with a harmonic shaker. The shaker is bolted to a force transducer, which is used to ensure that the shaker produces a constant force at each resonance frequency. A constant force of 0·8 N was used to drive the shell throughout the optimization and experiments.

The objective of the optimization problem is to minimize the sound power radiated by the half-cylindrical shell from its first five modes. To quieten the shell, two masses were affixed to its surface. The locations of the masses are determined by the optimization algorithm. Mathematically, the optimization problem can be written:

$$\text{Minimize}\{W_1 + W_2 + W_3 + W_4 + W_5\}, \tag{16}$$

where W_i is the sound power at the ith resonance frequency. The design variables are the locations of the two masses. The masses are small tungsten cylinders, each weighing 35·8 g. Tungsten was chosen because of its high density, in order that the masses might more closely approximate point masses. The value 35·8 g was chosen for convenience; i.e., masses of this weight were readily available from another experiment.

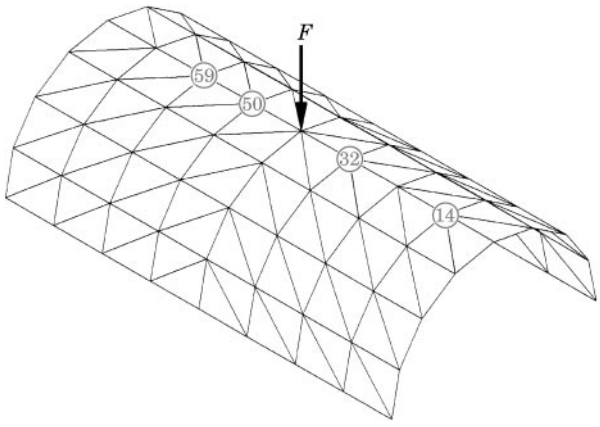

Figure 1. Finite element mesh for half-cylinder.

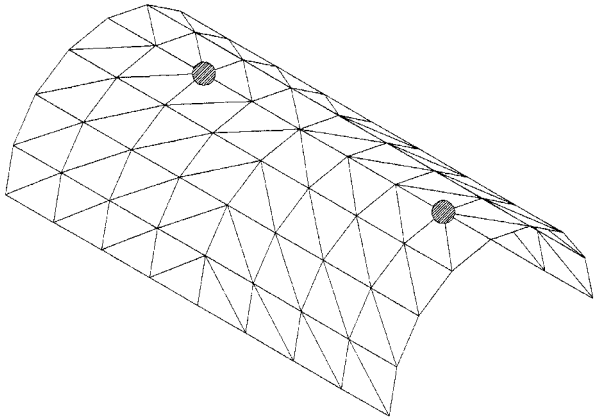

Figure 2. Optimal mass locations for half-cylinder.

3.1. OPTIMIZATION USING THE SOAR PROGRAM

To model the half-cylindrical shell, a finite element mesh was created with 81 nodes and 128 elements. Some of the more important node numbers are shown in Figure 1, as they will be referred to later. At the top center node a 19·0 g point mass was added, to simulate the mass of the moving part of the driver. The point masses were constrained to lie at nodal locations on the finite element mesh. A curvilinear co-ordinate system was mapped onto the finite element nodes so that each nodal location could be described by two co-ordinates: the distance along the long axis of the cylinder and circumferential location. Thus, each mass had two independent design variables, for a total of four.

Figure 2 shows the optimal locations for the point masses found by SOAR, at nodes 14, 59. *It is noteworthy that the optimal mass placement is asymmetric with respect to the transverse axis of the cylinder*, *even though the structure and excitation are symmetric*. The mode shapes of the shell before optimization are shown in Figure 3–7. The first mode shape (Figure 3) is called a "sway" mode; it radiates very little noise since the excitation force is in the vertical direction. The second mode (the "piston" mode shown in Figure 4) produces the largest amount of

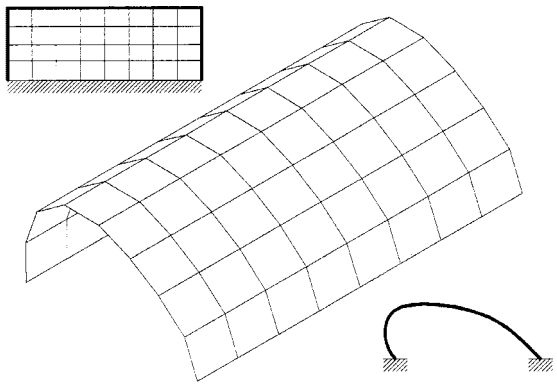

Figure 3. Mode 1—"sway" mode.

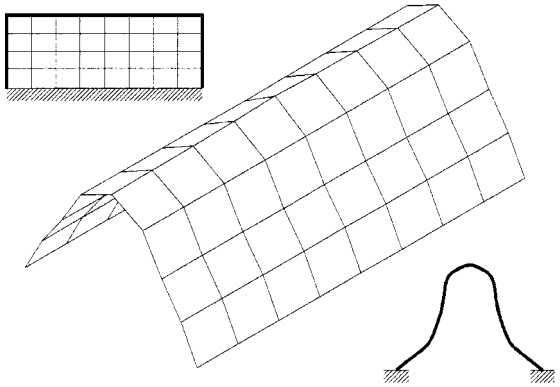

Figure 4. Mode 2—"piston" mode.

sound power. The third mode (the "rocking" mode shown in Figure 5) creates only a small amount of noise, due to the effect of volume velocity cancellation. That is to say, one side of the shell moves up and compresses the air while the other side moves downward and rarefies the same amount of air. The overall effect is that very little net volume velocity is created; i.e., the rocking mode behaves as a "weak radiator".

The fourth and fifth modes (shown in Figures 6 and 7) also create a small amount of noise due to volume velocity cancellation. They are included in the numerical portion of the analysis because "mode switching" was found to occur during optimization; that is, for certain mass placements a piston-type mode was the fourth eigenvalue extracted by inverse iteration, instead of the second. Thus, the fourth and fifth modes are kept in order to ensure that the optimal design is quiet over a fairly broad frequency range.

Table 1 shows the predicted results of optimization by the SOAR program. The first columns list the sound power and frequencies from the shell with no added masses, while the third shows the optimal sound power. The middle columns show the sound power results from the shell with the two masses in a "sub-optimal"

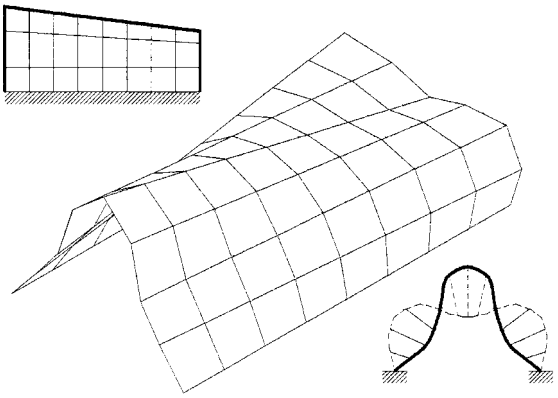

Figure 5. Mode 3—"rocking" mode.

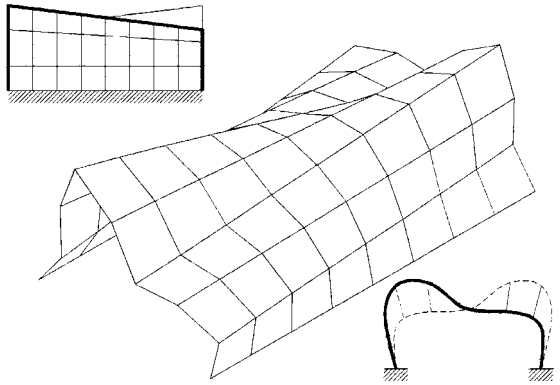

Figure 6. Mode 4—"rocking 2" mode.

location, at the nodes 32 and 50. All sound power measurements in this paper are given in decibels relative to 10^{-12} W.

After optimization, the asymmetric placement of mass along the ridge of the shell has the effect of converting the noisy "piston" mode into an asymmetric "rocking" type mode, which produces only a small amount of sound power. This is clearly seen in Figure 8, which shows the second and third mode shapes of the shell after optimization. Thus, the shell has been changed into a weak radiator, through the addition of only 71·6 g of mass ($\sim$8% of the total shell weight). The final result of this conversion is a 9·5 dB reduction in overall sound power at the first three modes.

The simulated annealing algorithm required 160 function evaluations, or 5% of the total design space, to converge to the optimal solution (one function evaluation consists of eigenvalue/vector extraction and sound power calculation for the first five modes.) However, convergence is strongly dependent upon the starting temperature, step size and other input parameters to the SA code, as well as the nature of the design space itself. For very large problems evaluation of 5% of the design space may be infeasible, but this quantity may be reduced by using a lower starting temperature and smaller initial step sizes. Of course, the higher the starting

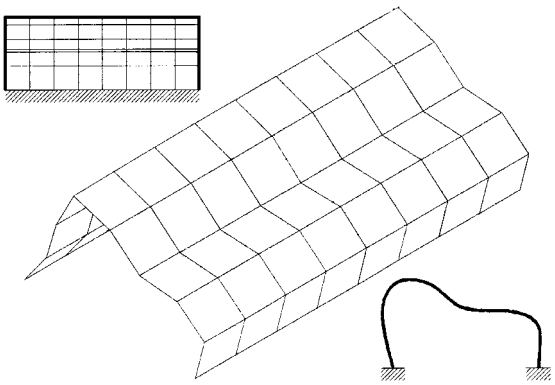

Figure 7. Mode 5—"piston 2" mode.

TABLE 1

Natural frequencies and sound power of shell before and after optimization

	No. masses		Sub-optimal masses nodes 32, 50		Optimal masses nodes 14, 59	
Mode	Freq (Hz)	Power	Freq (Hz)	Power	Freq (Hz)	Power
1	325·1	29·48	299·7	27·51	299·8	26·78
2	676·4	84·67	546·1	77·48	541·9	72·86
3	740·7	69·08	691·7	57·25	580·6	71·34
4	1184·3	62·45	1176·9	57·44	1139·9	57·17
5	1345·5	61·73	1345·5	57·12	1345·5	56·81
Total		84·83		77·60		75·31

temperature, the more confident a researcher may be in the "optimality" of the converged solution.

3.2. EXPERIMENTAL CONFIRMATION

The experimental analysis of the half-cylinder problem took place in two stages: modal analysis and acoustic intensity measurement. The division is due in large measure to the structure of the SOAR code itself, which is divided into the FEM vibration analyzer and the BEM sound power predictor. Experimental modal analysis and acoustic intensity measurements were performed for the half-cylinder without point masses, with the masses in their optimal locations and with the masses in the "sub-optimal" location (nodes 32, 50).

Modal analysis is necessary in order to confirm the results of the FEM code. Since the sound power produced by the structure is so strongly dependent upon its mode shapes, an inaccurate finite element code would yield incorrect sound power predictions. Acoustic intensity measurements are needed to confirm the results of the BEM sound power code.

3.2.1. *Experimental modal analysis*

The modal analysis experiments were performed using an impact hammer, a laser vibrometer, and the STAR Modal Analysis System software. The

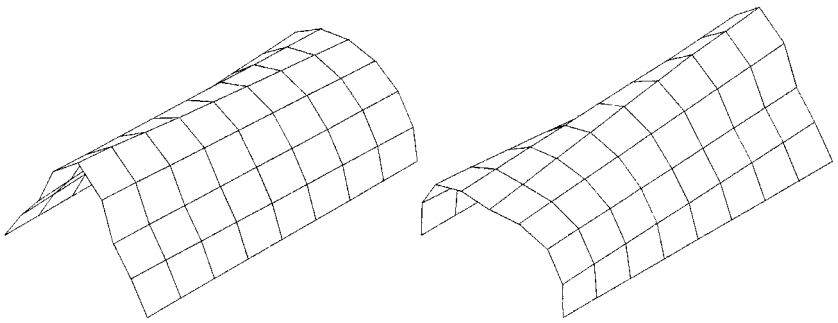

Figure 8. Second and third modes after optimization.

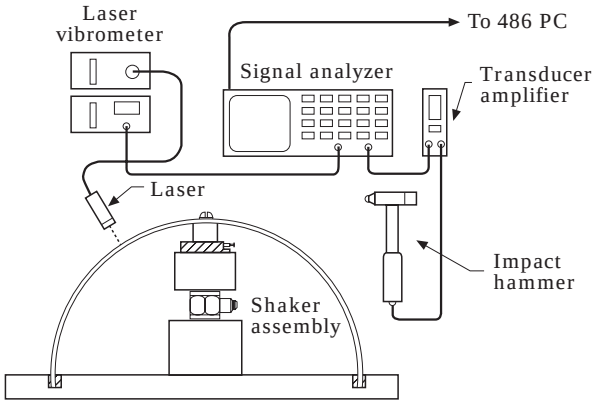

Figure 9. Experimental modal analysis apparatus.

experimental apparatus is shown in Figure 9. Of primary interest were the first few natural frequencies of the shell, and the mode shapes at these frequencies. The experimentally determined resonance frequencies of the first three modes are shown in Table 2, along with the predicted values. The largest discrepancy is 5·5%, which is good for a shell vibration problem. The mode shapes found by the STAR System were also in close agreement with those predicted by SOAR; that is, the shell clearly exhibited the "piston" and "rocking" modes at its second and third natural frequencies. The fourth and fifth modes were impossible to distinguish experimentally, due to the relatively small amount of displacement created by these modes.

3.2.2 *Acoustic intensity measurements*

The next set of experiments were undertaken to determine the accuracy of the SOAR sound power predictions. This was accomplished through the use of sound intensity measurements in a hemi-anechoic chamber. In the experiments, an HP 35660A dynamic signal analyzer was used to drive the harmonic shaker (through a power amplifier) with a pure tone at each of the first three resonance frequencies of the shell. The analyzer was also used to monitor the signal from the force transducer in the shaker assembly. This ensures that the shell is driven with a constant force at each frequency. Sound power measurements were made with the use of the HP 3569A Real Time Signal Analyzer in conjunction with a B & K Acoustic Intensity Probe.

TABLE 2

Predicted versus measured natural frequencies of shell (Hz)

Mode	No masses			Optimized		
	Predicted	Actual	% Diff	Predicted	Actual	% Diff
1	325	308	5·5	300	290	3·4
2	676	671	0·7	542	541	0·2
3	741	718	3·2	580	562	3·2

TABLE 3

Predicted versus measured sound power of shell (dB)

	No masses			Sub-optimal masses Nodes 32, 50			Optimal masses nodes 14, 59		
Mode	SOAR	Actual	Diff	SOAR	Actual	Diff	SOAR	Actual	Diff
1	29·48	36·00	6·52	27·51	40·22	12·71	26·78	36·47	9·69
2	84·67	82·84	1·83	77·48	79·84	2·36	72·86	72·91	0·05
3	69·08	68·94	0·14	57·25	56·25	1·00	71·34	70·17	1·17
Total	84·79	83·01	1·78	77·52	79·86	2·34	75·18	74·76	0·42

Owing to the difficulty of obtaining a constant force over a wide frequency range (the force varied by a factor of 3 over the range of 200–800 Hz with a constant voltage input) the shell was driven with a pure tone at each of its first three resonances. This approach has the added advantage of closely approximating SOAR, which also uses pure tone excitation at resonance. For each of the three aforementioned mass configurations (no masses, sub-optimal masses and optimal masses) the shell was driven at its first three natural frequencies and the radiated sound power was measured. The fourth and fifth modes were indistinguishable experimentally, and were not measured. As seen in Table 1, these modes are predicted to produce insignificant amounts of sound power relative to the second and third modes.

The sound power radiated by the shell as measured in the hemi-anechoic chamber is shown in Table 3. The sound power at the first resonance is not in agreement with the SOAR predictions because the predicted and measured sound power levels are very close to the noise floor in the test chamber. In fact, the sound produced by driving the shell at its first resonance with a force of 0·8 N was almost completely inaudible, except at very close range (within $\sim$30 cm). In practical terms, the large discrepancy between predicted and actual sound power levels for the first mode is unimportant, since so little noise is created by this mode.

On the other hand, accurate predictions for the second and third modes are important to this optimization problem, since they are the major noise producers in the frequency band of interest. As seen in Table 3, the predictions are in excellent agreement with the measured results, with a maximum discrepancy of 2·36 dB. Thus, the SOAR code is found to be an effective method of minimizing sound power for a vibrating shell structure.

As a final remark, it should be noted that the shell optimized in this study was a highly simplified structure. At low frequencies, the half-cylinder has a low modal density and the excitation force was easily determined *a priori*. The authors next task is to use SOAR on a more realistic engineering design problem, for example, a gearbox which is excited both structurally and acoustically.

4. CONCLUSION

A half-cylindrical shell structure driven with a point excitation force has been optimized for minimum sound power. The design variables were the locations of two 35·8 g tungsten "point" masses. The SOAR code found an asymmetric optimal solution for minimum sound power in the first three modes; the changing of a "strong radiator" mode shape into a "weak radiator" was found to be the key. Experimental confirmations of the predictions made by SOAR were carried out. Both experimental modal analysis and acoustic intensity measurements agreed closely with the SOAR predictions. In conclusion, the SOAR code was found to be an effective optimization routine capable of minimizing radiated sound power from a three-dimensional shell structure.

REFERENCES

1. M. A. Lang and C. L. Dym 1975 *Journal of the Acoustical Society of America* **57**, 1481–1487. Optimal acoustic design of sandwich panels.
2. J. S. Lamancusa 1988 *Journal of Sound and Vibration* **127**, 303–318. Geometric optimization of internal combustion engine induction systems for minimum noise transmission.
3. M. G. Milsted, T. Zhang and R. A. Hall 1993 *Proceedings of the Institution of Mechanical Engineers* **207**, 135–143. A numerical method for noise optimization of engine structures.
4. N. Vincent, P. Bouvet, D. J. Thompson and P. E. Gautier 1996 *Journal of Sound and Vibration* **193**, 161–171. Theoretical optimization of track components to reduce rolling noise.
5. R. J. Bernhard 1985 *Journal of Sound and Vibration* **98**, 55–65. A finite element method for synthesis of acoustical shapes.
6. C. Pal and I. Hagiwara 1993 *Finite Elements in Analysis and Design* **14**, 225–234. Dynamic analysis of a coupled structural–acoustic problem: simultaneous multimodal reduction of vehicle interior noise level by combined optimization.
7. S. P. Engelstad, 1995 *Proceedings of Inter-Noise* '95, Optimization strategies for minimum interior noise and weight using FEM/BEM.
8. A. D. Belegundu, R. R. Salagame and G. H. Koopmann 1994 *Structural Optimization* **8**, 113–119. A general optimization strategy for sound power minimization.
9. R. L. St. Pierre Jr and G. H. Koopmann 1995 *ASME Journal of Mechanical Design* **117**, 243–251. A design method for minimizing the sound power radiated from plates by adding optimally sized, discrete masses.
10. K. Naghshineh, G. H. Koopmann and A. D. Belegundu 1992 *Journal of the Acoustical Society of America* **92**, 841–855. Material tailoring of structures to achieve a minimum radiation condition.
11. K. Naghshineh and G. H. Koopmann 1994 *ASME Journal of Vibration and Acoustics* **116**, 31–37. An active control strategy for achieving weak radiator structures.
12. S. A. Hambric 1992 *Proceedings of the Fourth AIAA/USAF/NASA/OAI Symposium on Multidisciplinary Analysis and Optimization* 1096–1103. Structural–acoustic optimization of a point-excited submerged cylindrical shell.
13. S. A. Hambric 1995 *ASME Journal of Vibration and Acoustics* **117**, 136–144. Approximation techniques for broad-band acoustic radiated noise design optimization problems.
14. S. A. Hambric 1996 *ASME Journal of Vibrations and Acoustics* **118**, 529–532. Sensitivity calculations for broad-band acoustic radiated noise design optimization problems.

15. A. J. KEANE 1994 *Adaptive Computing in Engineering Design and Control* 14–27. Experiences with optimizers in structural design.
16. S. SZYKMAN and J. CAGAN 1995 *ASME Design Engineering Technical Conferences* **1**, 431–438. Synthesis of optimal non-orthogonal routes.
17. S. SZYKMAN and J. CAGAN 1995 *ASME Journal of Mechanical Design* **117**, 308–314. A simulated annealing-based approach to three-dimensional component packing.
18. R. D. COOK, D. S. MALKUS and M. E. PLESHA 1989 *Concepts and Applications of Finite Element Analysis*. New York: John Wiley; third edition.
19. O. C. ZIENKIEWICZ 1983 *The Finite Element Method*. New York: McGraw-Hill; third edition p. 329.
20. T. R. CHANDRUPATLA and A. D. BELEGUNDU 1991 *Introduction to Finite Elements in Engineering*. Englewood Cliffs, NJ: Prentice-Hall; p. 343.
21. G. H. KOOPMANN, L. SONG and J. B. FAHNLINE 1989 *Journal of the Acoustic Society of America* **86**, 2433–2438. A method for computing acoustic fields based on the principle of wave superposition.
22. J. B. FAHNLINE and G. H. KOOPMANN 1996 *Journal of the Acoustical Society of America* **100**, 3539–3547. Lumped parameter model for the acoustic power output from a vibrating structure.
23. H. LEVINE 1980 *Journal of the Acoustical Society of America* **67**, 1935–1946. Output of acoustical sources.
24. H. LEVINE 1980 *Journal of the Acoustical Society of America* **68**, 1199–1205. On source radiation.
25. A. CORANA, 1987 *ACM Transactions on Mathematical Software* **13**, 262–280. Minimizing multimodal functions of continuous variables with the "Simulated Annealing" algorithm.